Maximizing annual yield of bifacial photovoltaic noise barriers

Faturrochman, G.J.; de Jong, M.M.; Santbergen, R.; Folkerts, W.; Zeman, M.; Smets, A.H.M.

DOI
10.1016/j.solener.2018.01.001

Publication date
2018

Document Version
Accepted author manuscript

Published in
Solar Energy

Citation (APA)
Faturrochman, G. J., de Jong, M. M., Santbergen, R., Folkerts, W., Zeman, M., & Smets, A. H. M. (2018). Maximizing annual yield of bifacial photovoltaic noise barriers. *Solar Energy*, *162*, 300-305. https://doi.org/10.1016/j.solener.2018.01.001

Maximizing annual yield of bifacial photovoltaic noise barriers

G.J. Faturrochman[a,b], M.M. de Jong[b], R. Santbergen[a], W. Folkerts[b], M. Zeman[a], A.H.M. Smets[a]

[a] *Photovoltaic Materials and Devices, Delft University of Technology, Mekelweg 4, 2628 CD Delft, The Netherlands*

[b] *Solar Energy Application Centre (SEAC), High Tech Campus 21, 5656 AE Eindhoven, The Netherlands*

Abstract

In this work we consider noise barriers with integrated photovoltaic modules. The novelty is that *bifacial* modules are considered. A full scale bifacial photovoltaic noise barrier was built and its power output was monitored. In addition we developed an advanced numerical model for predicting this power output for given weather conditions. Excellent agreement was found between the measured power output and the model prediction. Next we used this model to demonstrate the effects of the orientation, tilt, location, cell position and bypass-diode configuration on the annual energy yield of bifacial photovoltaic noise barriers.

Keywords: photovoltaic, BIPV, bifacial, noise barrier, annual energy yield

1. Introduction

Noise barriers shield urban areas from road noise. Combining these noise barriers with photovoltaic (PV) modules is an elegant way to integrate renewable electricity generation in the built environment. The first so-called photovoltaic noise barriers were already installed in 1989 in Chur, Switzerland (Nordmann and Goetzberger, 1994). In this design conventional PV modules are simply placed along a road. In the 1990's a number of pilot installations were built, mostly in Switzerland, Germany (Nordmann et al., 2002) and the Netherlands (Dutch Ministry of Infrastructure and the Environment, 1995; Betcke et al., 2002). After these initial pilot projects, much larger solar noise barriers were built with examples in Italy, where a 730 kWp and a 833 kWp photovoltaic noise barrier were erected in 2009 and 2010. Recently even larger photovoltaic noise barriers, ranging from 1 MWp to 2.065 MWp were built in several places in Germany, e.g. in Toging am Inn, Wallersdorf, Polling and Aschaffenburg.

In recent years the emphasis has shifted to designs with the PV module seamlessly integrated in the noise barrier structure. This improves the aesthetics and shortens construction time. However, the orientation of the PV module is inherently dictated by the direction of the road and its tilt usually is near-vertical. This sub-optimum orientation and tilt can significantly reduce the annual yield of conventional *monofacial* PV modules. However, *bifacial* PV modules, which have a transparent rear side such that the cells can convert both the light incident on their front and on their rear into electricity, are more resilient (Yusufoglu et al., 2015; Shoukry et al., 2016) and seem more promising for application in noise barriers.

The first *bifacial* noise barrier was built on a highway bridge in Aubrugg near Zurich, Switzerland in 1997 and extended in 2004 (Nordmann et al., 2002). Together with a bifacial photovoltaic noise barriers along a railway in Münsingen, Switzerland, these installations, are the only bifacial photovoltaic noise barriers to date. Both installations are facing East and West and are placed vertical. More information and a summary of their measured performance is given by Nordmann et al. (2012) and by Vontobel (2009). In the Netherlands, the National Road Authority plans to build a 450 m long bifacial photovoltaic noise barrier in the city of Uden in 2018 (Dutch Ministry of Infrastructure and the Environment, 2017).

The integration of bifacial PV modules into a noise barrier also comes with challenges. The barriers require a thick noise absorber, implying that the conventional module glass thickness has to be increased from 3 to 8 mm, both at the front and rear. This, combined with the required resistance to wind loads, means that bulky support structures are necessary. These structures can cast a shadow on the rear surface of the bifacial module (de Jong et al., 2016).

Numerical simulation is an important tool for predicting the power output and annual yield of a PV system and allows its optimization for a particular location. Several software packages are available for predicting the annual yield of conventional PV systems (Sauer et al., 2015). However, for near-vertical systems yield calculation is more complex as the albedo component, representing the irradiance on the PV module due to reflections from the ground, plays a more important role. The calculation becomes especially complex when *bifacial* PV systems are considered, as both the irradiance on front and rear side of the PV module has to be calculated. This requires a novel type of optical model. Also the thermal and electrical models need to be adapted for application to bifacial modules.

In this work, we present an advanced numerical model

for predicting a bifacial PV system's power output for given weather conditions. We apply the model to a PV noise barrier for the first time. The model is validated experimentally by comparing the simulated and measured power output. Next we used this model to demonstrate the effects of orientation, tilt, location, cell position and bypass-diode configuration on the annual energy yield of the bifacial photovoltaic noise barrier.

2. Model

In this section we present the modeled geometry of the bifacial photovoltaic noise barrier and the optical, thermal and electrical models used to determine its energy yield. Meteorological data such as direct and diffuse irradiance, sun position, ambient temperature and wind speed for a typical year on a basis of 10 minutes is used as input (Meteonorm, 2015). From this the incident plane of array irradiance, module temperature and power output are calculated at every time step.

2.1. Reference design

Our photovoltaic noise barrier design follows the standard modular noise barrier design published by the Dutch Ministry of Infrastructure and the Environment (Rijkswaterstaat, 2006). According to this regulation, the noise barriers should not be tilted more than 15° from vertical to maintain the noise reducing functionality. Our noise barrier reference design and its dimensions are shown in Fig. 1. It contains eight bifacial PV modules, each consisting of 48 series connected mono-crystalline bifacial solar cells manufactured by Neo Solar Power. These cells have an STC efficiency of 19.6% when illuminated from the front and 18.2% when illuminated from the rear. Note that the ratio between front and rear efficiencies is called the bifaciality factor which in this case is 0.93. The bifacial cells are sandwiched between two 8 mm-thick glass plates. There is a margin of approximately 20 cm between the outer cells and metal frame surrounding the noise barrier. The cell spacing of the module is 16 mm. This frame protrudes 50 cm at the rear side. The frame needs to be this thick in order to handle the mass of the barrier itself as well as the additional load induced by the wind.

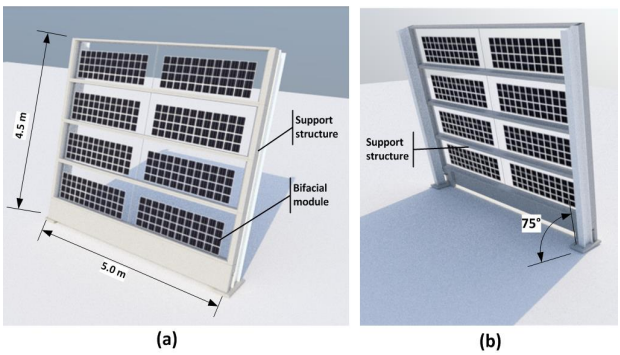

Figure 1: Computer rendering of one section of bifacial photovoltaic noise barrier containing 4 × 2 modules, each with 4 × 12 cells of 15 × 15 cm. Front view (a) and rear view (b).

2.2. Optical model

The optical model calculates the incident irradiance on both front and rear of the PV cells for every 10 minute time step, taking into account direct, diffuse and albedo components. *Direct* irradiance is calculated from the direct normal irradiance (DNI), obtained from Meteonorm, taking into account the sun position and reflection and parasitic absorption losses from the glass (De Soto et al., 2006). The shadow cast by the frame protruding at the rear is also taken into account. Fig. 2 represents the rear side of the top right module in a West facing photovoltaic noise barrier. Each square represents a cell and the dark bands indicate the shadows on a summer day at 8 AM and 10 AM. The number indicates the percentage of the cell area that is shaded, which varies from 0 (unshaded) to 100 (fully shaded).

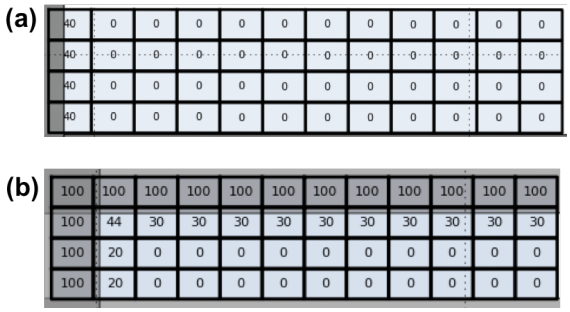

Figure 2: Shadow cast by frame on rear side of a bifacial PV module during summer day as calculated by the optical model. The numbers indicate the cell shading fraction. (a) 8 AM (b) 10 AM.

The *diffuse* component is calculated using the Perez transposition model (Perez et al., 1990), taking the diffuse horizontal irradiance (DHI) from Meteonorm as input. The Perez transposition model takes into account the circumsolar light, horizon brightening and sky view factor of the module. The slight reduction in sky view factor for cells at the rear side due to the protruding frame is taken into account.

The *albedo* component representing the ground reflected irradiance is calculated using the view factor of the ground. For every time step the outline of the shadow of the noise barrier on the ground is calculated and the view factor from each cell to this shadow is determined. This allows taking into account the fact that there is no reflected direct irradiance from the shaded part of the ground. This is important for accurately calculating rear side irradiance on a bifacial PV module (Yusufoglu et al., 2015).

2.3. Thermal model

The thermal model calculates the cell temperatures based on the incident irradiance and the ambient temperature. In this work, the thermal model for glass-glass PV modules by Notton et al. (2005) is used. The model takes into account conductive, convective and radiative heat transfer between front glass, solar cell, rear glass and the ambient. The model was extended to account for the additional heat generated by irradiance being absorbed from the rear side of the bifacial solar cells. The influence of the wind speed on the convective heat transfer

coefficient is taken into account by using the expression given by McAdams (1954). The radiative heat exchange of the noise barrier with both sky and ground is considered. The glass' emissivity is assumed to be 0.85 and its conductivity is set to 1 $W/(m \cdot K)$. The c-Si solar cells have a much higher conductivity of 149 $W/(m \cdot K)$ (Bloem et al., 2000).

2.4. Electrical Model

The electrical model calculates the current-voltage characteristics (I-V curve) of the PV modules every time step. The effect of non-uniform irradiance and temperature are taken into account. Each PV cell is represented as a two-diode equivalent circuit (Smets et al., 2016). The current generated by the current source is set proportional to the irradiance on the cell with a proportionality constant of 8.6 $mA/(W/m^2)$. The rear irradiance is multiplied by the bifaciality factor of 0.93 before adding its current contribution. The cell temperature affects the diode characteristics through the thermal voltage in the exponent of the diode equation. The resistance values are extracted by fitting the I-V curve under standard test conditions. All equivalent circuits, each representing one PV cell, are then connected in series to form an entire PV module. In addition, bypass diodes can be connected in various configurations, as will be discussed in section 3.3.3. Finally, the overall I-V curve is calculated. From this, the power output is obtained.

2.5. Experimental validation of the model

One section of the bifacial photovoltaic noise barrier was built and its power output was monitored. To validate the model, the calculated power output was compared to this measured power output.

2.5.1. Experimental setup

A prototype of the bifacial photovoltaic noise barrier was built in Den Bosch, the Netherlands (51.69°N, 5.30°E). As shown in Fig. 3, the barriers consist of three different technologies:luminescent solar concentrator (row 1 and 2), bifacial PV modules (row 3) and monofacial PV modules (row 4). In this work we consider only the part with the bifacial modules, which is identical to the corresponding part of the reference design (see section 2.1). The noise barrier has West orientation. The bifacial solar cells mentioned in section 2.1 are used. The irradiance in the plane of array (G_{POA}) was measured simultaneously on both front and rear side using two pyranometers. A third pyranometer measured the global horizontal irradiance (GHI). The wind speed and ambient temperature were measured using a weather station. In addition, an EKO instrument MP-160 I-V curve tracer was installed to measure the I-V response of the bifacial modules.

2.5.2. Comparison of measurement and simulation

A bifacial photovoltaic noise barrier with the exact dimensions and orientation as described above was simulated using the model described in section 2. The meteorological conditions GHI and ambient temperature, measured on site, were used as input. The direct and diffuse irradiance components were obtained from the measured plane of array irradiance using the Reindl separation model (Reindl et al., 1990). Finally, the shading factor obtained using the model explained in section 2.2 was incorporated in the irradiance calculation.

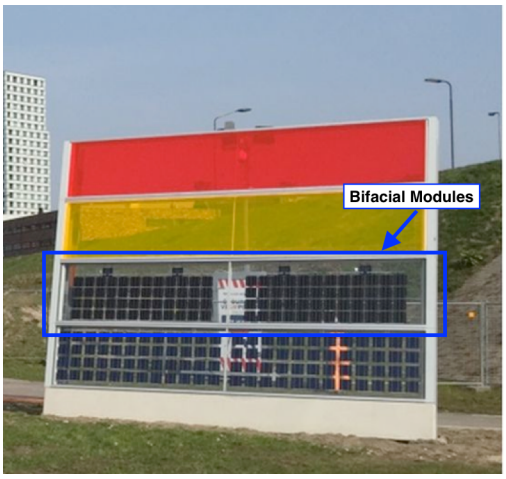

Figure 3: Prototype of photovoltaic noise barrier test setup in Den Bosch, the Netherlands. The bifacial part considered here is indicated.

Fig. 4 shows the simulated power output (blue line) and the measured power output (red line). The top, middle and bottom figure represent a sunny, partly cloudy and overcast day, respectively. The model predicts that on a sunny day the power output shows a double peak (see blue line in Fig. 4a). This is because in the early morning and in the late afternoon the West-facing bifacial module is illuminated from rear and front, respectively. During the overcast day the simulated power output is rather low and constant throughout the day, while during the partly cloudy day the power output fluctuates. The measured power output (red line) shows very good agreement with the simulated power output (blue line), indicating that the model can accurately predict the power output for a wide range of weather conditions.

3. Simulation results

With the model validated, it can be used to predict the power output for an entire year to determine the annual yield. The model was used to study the effect of design changes on this yield. The starting point is the reference design explained in section 2.1. In this work, we present the average of total yield of all eight modules in the barrier, expressed in kWh/kW_p.

3.1. Effect of orientation and tilt

We simulate the annual yield of the bifacial photovoltaic noise barrier as a function of its orientation and tilt angle, without changing other parameters. Eight different orientations were considered and for each orientation the tilt angle from the vertical was varied between 0 and 15°. First we perform these simulations using the meteorological conditions of Amsterdam, the Netherlands as input. The results are shown in Fig. 5a, with the red triangles corresponding to the standard tilt of 15°. This reveals that the South orientation, with the front of the bifacial modules facing South,

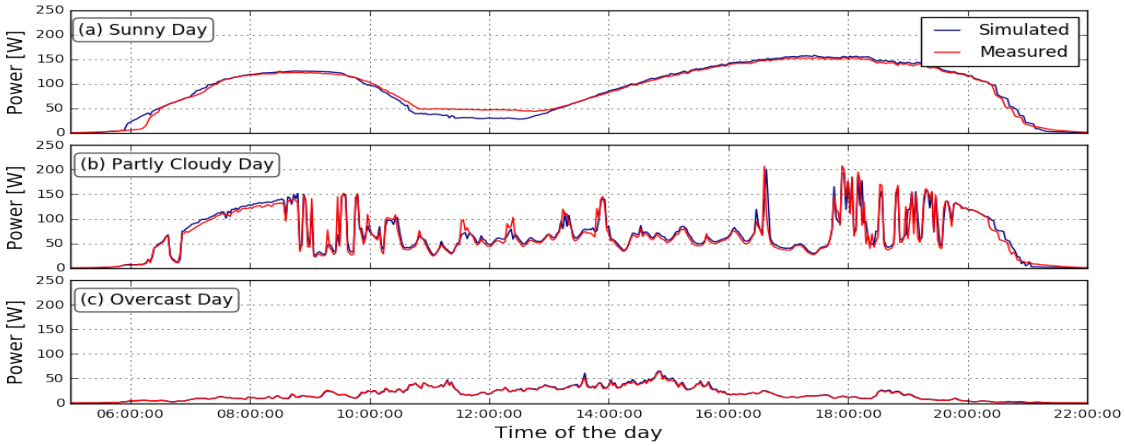

Figure 4: Simulated and measured power output during (a) sunny day, (b) partial cloudy day, (c) overcast day.

gives the highest annual yield of up to 1100 kWh/kW$_p$. The north facing bifacial noise barrier still has an annual yield of 800 kWh/kW$_p$. A *monofacial* barrier with North orientation would have a very low annual yield of 300 kWh/kW$_p$ (not shown). Finally, decreasing the tilt angle, i.e. placing the barrier more vertical, decreases the yield of a South facing barrier but increases the yield of a North facing barrier.

3.2. Different geographical locations

Next, the simulation is repeated with the meteorological data of three different geographical locations: Dubai (25.20°N, 55.27°E), Jakarta (6.17°S, 106.86°E), and Melbourne (37.81°S, 144.96°E). The result for Dubai (Fig. 5b) show roughly the same trends as for Amsterdam. Because it is a more sunny location the yield is as high as 1600 kWh/kW$_p$. The results for Jakarta, which is close to the equator, are shown in Fig. 5c. Interestingly, this shows that a relatively high annual yield of close to 1400 kWh/kW$_p$ is obtained for East or West oriented bifacial photovoltaic noise barriers. A (near) vertical *monofacial* PV module close to the equator would achieve only 700 kWh/kW$_p$. This is because any vertical module will receive little irradiance when the sun is near zenith, i.e. around noon. With East or West orientation it can receive a relatively high irradiance for either the first 4 hours after sunrise or the last 4 hours before sunset. However, an East or West oriented *bifacial* PV module can receive irradiance during both of these times, resulting in a relatively high annual yield. Finally, the results for Melbourne are shown in Fig. 5d. These results are somewhat similar to those of Dubai, but with the roles of North and South orientation reversed as expected for a location in the southern hemisphere.

3.3. Mitigating cell shading by the frame

As can be seen from Fig. 1, the frame supporting the noise barrier protrudes at the rear side. When the sun illuminates the rear side of the bifacial noise barrier under a large angle of incidence, this frame can cast a shadow on the rear of the bifacial PV cells. For example, Fig. 2 shows that for a West oriented barrier in the morning the rear side of the edge cells, the cells nearest to the frame, are shaded. In this section the effect of this shading loss on the annual yield is quantified. For this, we consider the reference design in one location (Amsterdam), with a fixed tilt angle of 15° at eight orientations. In this case, we keep the size of the frame fixed. First we quantify the shading losses and then investigate two ways to reduce them: i) placing cells in different locations and ii) adding bypass diodes.

3.3.1. Rear side shading loss

The red bars in Fig. 6 show the annual yield of the reference design in Amsterdam with 15° tilt for every orientation, as already shown in Fig. 5a (red triangles). To quantify the shading losses these simulations were repeated for the same noise barrier but without the frame, and therefore without the shading by the frame. The results are indicated by the gray bars. In every orientation the yield with frame (red) bars is lower than the yield without frame (gray bars). The difference indicates the shading loss. This shows that for a South oriented barrier, the shading loss is negligible. On the other hand, for a North oriented barrier 13.3% of the annual yield is lost due to shading by the frame. This is mainly because in that case the bifacial PV modules receive most of the direct irradiance on their rear side, where frame protrudes and can cast a shadow on the cells. Note that the frame is required to provide the structural support and can not be reduced in size.

3.3.2. Cell position

The simulations were repeated with the frame, but with two alternative cell layouts. In the first layout the spacing between the cells is increased to approximately 5 cm, similar to the layout shown in the bottom row of the test setup, shown in Fig. 3, with only 1 cm away from the sides. The consequence of this is that the cells near the edge are closer to the frame. In the second layout, the spacing between the cells is reduced to 10 mm and all cells are placed as far away from the frame as possible. The annual yield was also simulated for the alternative cell layouts and the results are shown in Fig. 6. This shows that with the broad cell placement (blue bars) the annual yield is lower, i.e. the shading loss is larger. For the narrow cell placement (green bars) the yield is somewhat

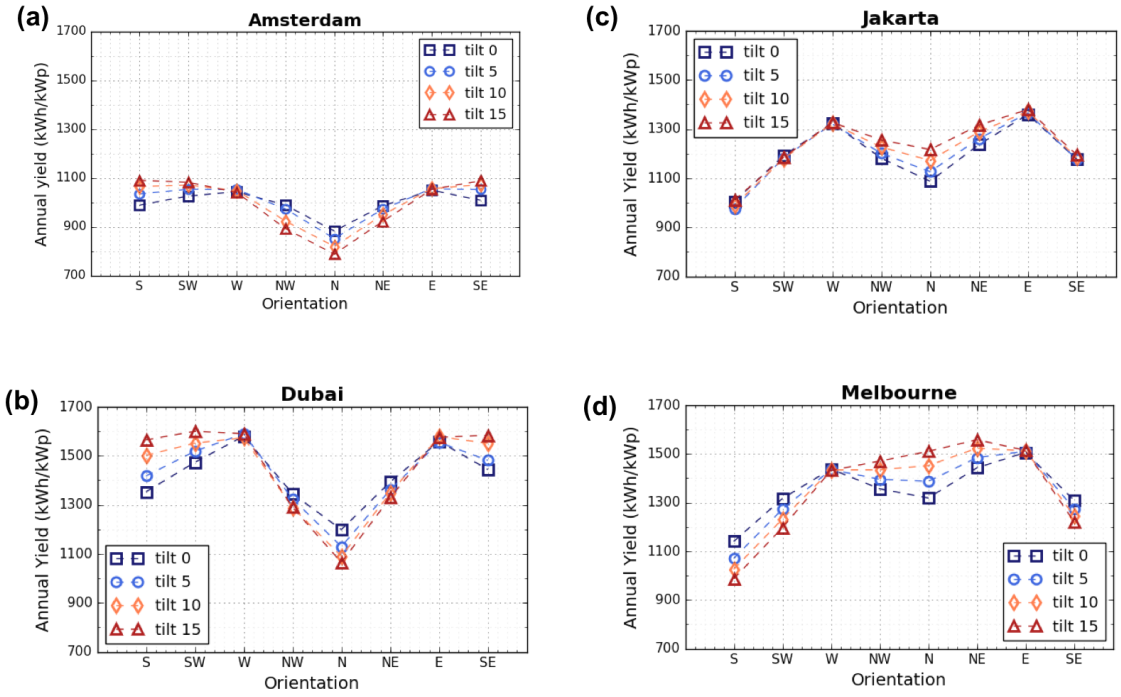

Figure 5: Simulated annual yield of bifacial PV noise barrier as a function of orientation and tilt angle from vertical, for a) Amsterdam, b) Dubai, c) Jakarta, d) Melbourne.

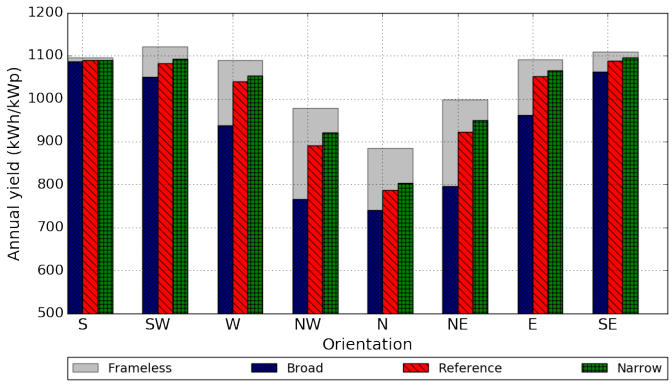

Figure 6: Simulated annual yield as a function of orientation for broad, reference and narrow cell placement. The simulated yield without shading from the frame is indicated in gray.

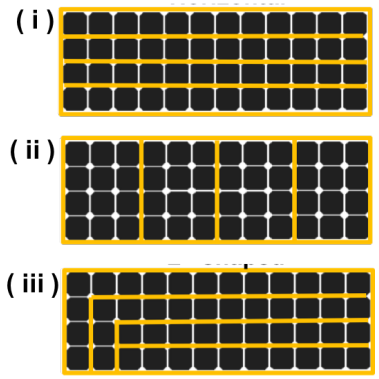

Figure 7: Three different bypass diodes interconnections (i) one diode per row (ii) one diode per three column and (iii) diodes in L-shaped configuration.

higher and the shading losses are reduced to 11.3% for the north oriented barrier. This confirms that when the cells are further from the protruding frame, cell shading occurs less frequently.

3.3.3. Bypass diode configuration

A common way to reduce shading losses is the application of bypass diodes that can guide the current around a (partly) shaded cell. It is generally too expensive to equip every PV cell with a bypass diode and one bypass diode is generally applied per several rows or columns of cells. The PV modules applied in the noise barrier have 12 columns of 4 cells. We consider three different configurations, shown in Fig. 7, each requiring four bypass diodes: i) one diode per row, ii) one diode per 3 columns, iii) one diode per L-shape. Here the L-shape consists of one row and one column as indicated.

The annual yield for a North-oriented noise barrier is simulated with each of the bypass diode configurations. The results are shown in Fig. 8, where the bar labeled 'ref' is the reference case without bypass diodes with a shading loss of 13.3%. Diode configurations reduce this shading loss to 11.9% (row), 11.2% (column) and 10.7% (L), respectively. Note that simulations with more than 4 bypass diodes have also been performed and it turns out that more than 12 bypass diodes are required to reduce the shading loss to less than 10% (not shown).

4. Conclusions

In this work we considered bifacial photovoltaic noise barrier. To analyze their performance, we developed a detailed optical, thermal and electrical model that takes the meteorological data as input and predicts the power output and annual energy yield. This model was shown

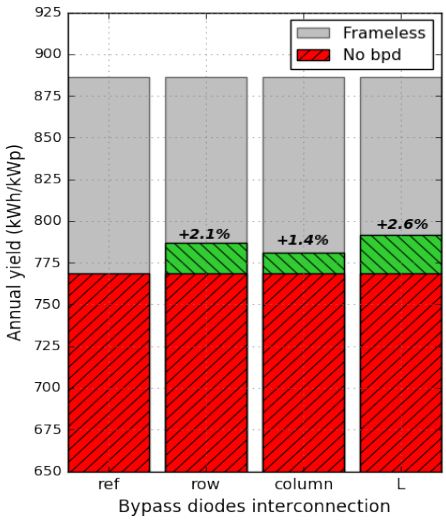

Figure 8: Simulated annual yield of north-facing bifacial PV noise barrier for different bypass diodes configurations, each requiring 4 diodes per module.

to be accurate by comparing the predicted power output to the power output measured on a prototype bifacial photovoltaic noise barrier under different weather conditions. The model was then used as a tool to predict the annual energy yield of a bifacial photovoltaic noise barrier for different orientations, tilt angles, cell positioning and bypass diode layout.

Interestingly, near the equator (we considered Jakarta) the highest annual yield is obtained for a barrier oriented East or West, such that it can receive direct irradiance from both front and rear in the early morning and late afternoon. Further North (we considered Dubai and Amsterdam) East or West orientations still perform well, but the highest annual yield is obtained when the front of the bifacial photovoltaic noise barrier faces South. However, because also the irradiance incident from the rear can be converted to electricity, a North facing barrier still achieves an annual yield of 70 to 90% of the maximum achievable yield.

The protruding frame casts a shadow on the rear side of the bifacial cells. Our simulations show that this reduces the annual yield by 13.3%. This shading loss can be reduced to 11.3% by placing the PV cells further from the protruding frame or to 10.7% using four bypass diodes in a novel L-shape configuration.

Aknowledgement

This work is supported by Netherlands Enterprise Agency (RVO) via TKI-ZEGO project SONOB with grant number TEZG114009 and TKI Urban Energy project ANTILOPE with grant number TEID215011.

References

Betcke, J., van Dijk, V., Alsema, E., 2002. Opbrengstgegevens van het PV-geluidsscherm langs de A27 na twee jaar systeembedrijf. Tech. Rep. NWS-E-2002-14, Copernicus Instituut, Universiteit Utrecht.

Bloem, J., Zaaiman, W., Bucci, C., Nacci, V., 2000. Proposal for a PV reference module and a test reference environment for bipv applications. In: European Photovoltaic Solar Energy Conference. pp. 1922–1925.

de Jong, M., van den Donker, M., Folkerts, W., 2016. Self-shading in bifacial photovoltaic noise barriers. In: 32nd European Photovoltaic Solar Energy Conference (EUPVSEC).

De Soto, W., Klein, S. A., Beckman, W. A., 2006. Improvement and validation of a model for photovoltaic array performance. Solar Energy 80, 78–88.

Dutch Ministry of Infrastructure and the Environment, 1995. Geluidsscherm a27. http://www.pvdatabase.org/pdf/Geluidsscherm_A27.pdf.

Dutch Ministry of Infrastructure and the Environment, 2017. Solar highways. http://solarhighways.eu/en.

McAdams, W., 1954. Heat Transmission, 1st Edition. McGraw-Hill.

Meteonorm, 2015. Meteonorm Software.

Nordmann, T., Frölich, A., Clavadetscher, L., 2002. Drei integrierte PV-Schallschutz Versuchsfelder: Bau und Erprobung. Tech. rep., TNC Consulting AG.

Nordmann, T., Goetzberger, A., 1994. Motorway sound barriers: recent results and new concepts for advancement of technology. In: 1st World Conference on Photovoltaic Energy Conversion (WCPEC). Vol. 1. IEEE.

Nordmann, T., Vontobel, T., Clavadetscher, L., 2012. 15 Years of Practical Experience in Development and Improvement of Bifacial Photovoltaic Noise Barriers Along Highways and Railway Lines in Switzerland. In: 27th European Photovoltaic Solar Energy Converence and Exhibition. p. 5DO.7.2.

Notton, G., Cristofari, C., Mattei, M., Poggi, P., 2005. Modelling of a double-glass photovoltaic module using finite differences. Applied Thermal Engineering 25 (17-18), 2854–2877.

Perez, R., Seals, R., Zelenka, A., 1990. Climatic Evaluation of Models that Prdict Hourly Direct Irradiance From Hourly Global Irradiance. Solar Energy 44 (2), 99–108.

Reindl, D., Beckman, W., Dufie, J., 1990. Difuse Fraction Correlation. Solar Energy 45 (1), 1–7.

Rijkswaterstaat, 2006. Modulaire Geluidsschermen (Modular Noise Barrier).

Sauer, K. J., Roessler, T., Hansen, C. W., 2015. Modeling the irradiance and temperature dependence of photovoltaic modules in pvsyst. IEEE Journal of Photovoltaics 5, 152 – 158.

Shoukry, I., Libal, J., Kopecek, R., Wefringhaus, E., Werner, J., 2016. Modelling of Bifacial Gain for Stand-alone and in-field Installed Bifacial PV Modules. In: 6th International Conference on Silicon Photovoltaics, SiliconPV 2016. Vol. 92. pp. 600–608.

Smets, A. H., Jäger, K., Isabella, O., van Swaaij, R. A., Zeman, M., 2016. Solar Energy, the Physics and Engineering of Photovoltaic Conversion Technologies and Systems, 1st Edition. UIT Cambridge Ltd, Cambridge.

Vontobel, T., 2009. Bifacial photovoltaik schallschutz anlage im sbb bahnhof münsingen. Tech. rep., TNC Consulting AG.

Yusufoglu, U. A., Pletzer, T. M., Koduvelikulathu, L. J., 2015. Analysis of the Annual Performance of Bifacial Modules and Optimization Methods. IEEE Journal of Photovoltaics 5, 320–328.